IOP Conf. Series: Materials Science and Engineering **310** (2018) 012095 doi:10.1088/1757-899X/310/1/012095

Numerical Investigation of Ice Slurry Flow in a Horizontal Pipe

K S Rawat[1], A K Pratihar[2]
[1,2]Department of Mechanical Engineering, G.B. Pant University of Ag. & Technology, Pantnagar-263145, Uttarakhand, India

E-mail: kamalrawat273@gmail.com

Abstract. In the last decade, phase changing material slurry (PCMS) gained much attention as a cooling medium due to its high energy storage capacity and transportability. However the flow of PCM slurry is a complex phenomenon as it affected by various parameters, i.e. fluid properties, velocity, particle size and concentration etc.. In the present work ice is used as a PCM and numerical investigation of heterogeneous slurry flow has been carried out using Eulerian KTGF model in a horizontal pipe. Firstly the present model is validated with existing experiment results available in the literature, and then model is applied to the present problem. Results show that, flow is almost homogeneous for ethanol based ice slurry with particle diameter of 0.1 mm at the velocity of 1 m/s. It is also found that ice particle distribution is more uniform at higher velocity, concentration of ice and ethanol in slurry. Results also show that ice concentration increases on the top of the pipe, and the effect of particle wall collision is more significant at higher particle diameter.

1. Introduction

The world energy consumption is increasing with the growth of the economy and population. Currently, 80% energy needs of the world are being fulfilled by the non-renewable energy resources (crude oil, coal and gas), which are depleting rapidly [1]. The electricity consumed by the HVAC&R systems accounts for a large portion of the total world electricity consumption [1-2]. Meanwhile, the world is also facing the environmental challenges due to the emission of the synthetic refrigerants like CFCs and HCFCs. Phase change material slurry (PCMS) as a secondary loop refrigerant can be used to reduce the energy consumption and the system charge. PCMS can store a greater amount of thermal energy per unit volume than single phase fluid. Thus, it reduces system charge and consumes less pumping power. PCMS can be produced during off-peak electricity load and supplied during peak load of electricity, which helps to balance the demand and supply of electricity [3].

PCMS is a multiphase fluid or mixture of liquid and solid particles of a PCM. PCMS may comprise of ice, clathrate hydrate, paraffin wax or carbon dioxide as dispersed solid particles in a carrier liquid as a secondary loop refrigerant. Selection of PCMS depends on the desired operating temperature range and its chemical (level of flammability, toxicity and corrosiveness) and physical (vapour pressure and phase segregation) properties for particular applications [4]. Among the different PCMS, ice slurry is an appropriate choice for food and air-conditioning application. Ice slurry has a high energy storage density, high heat transfer coefficient and it also reduces the system size (storage tank and pipelines)

[1] kamalrawat273@gmail.com

[5]. Due to these attractive features, the ice slurry gains much attention as a secondary loop refrigerant over other alternatives. Ice slurry can be defined as a dispersed ice particles in a carrier liquid (either water or a binary solution of water and freezing point depressant). Based on the application, the initial size of the particle (0.1-1.0 mm), their concentration (10-30 % volume fraction) and the configuration of carrier liquid may vary in the ice slurry [6].

As the flow of ice slurry through a pipe is a complex S-L flow, it is a formidable task to analyse this type of flow by experiments due to complexities in measurements and visualization caused by dispersed solid particles. In such cases, Computational fluid dynamics (CFD) is a practical and cost-worthy approach which provides ample information about the flow, especially pressure drop, velocity and particle concentration profile [7]. The pressure drop and particle concentration profile are important factors in the solid-liquid flow, to determine the pump capacity and the effect of other parameters (particle diameter, initial solid volume fraction, concentration of FPD) which affect the mixture and solid flow rates, as well as subservient effects like particle deterioration and wall abrasion [8]. Some attempts have been already made to solve such type of problems through CFD [9-15], however, still quantitative literature is not available for modelling on ice slurry.

Modeling of dense solid-liquid (S-L) flow requires knowledge of the flow field around each particle, interaction between particles, particles and the wall, along with their effect on the liquid. To computational solution for such problem, we have two approaches: Euler-Lagrange (E-L) and Euler-Euler (E-E). In E-L approach, liquid phase is treated as continuum to solve and solid phase is solved by tracking a large number of solid particles in the flow field. The principle drawback of the E-L approach is that it ignores the collision interaction between solid particles, furthermore in dense flow too many particles have to be tracked and computational time increases with the number of particles. The Euler-Euler approach considers both solid and liquid phases in a continuum that interpenetrates each other and exchange momentum, hence this technique also known as the interpenetrating continua model. In E-E approach, computational time doesn't increase with particle concentration. In this approach, each conservation equation is solved for both phases separately [16].

In E-E approach three different models: VOF, mixture and Eulerian model are available. However Eulerian model with Kinetic theory of granular flow (KTGF) is the most appropriate model to solve such solid-liquid flow. In the present work, numerical investigation of the PCM slurry flow has been carried out using Eulerian KTGF model in a horizontal pipe of 23 mm diameter and 2 m length. Ice is used as a PCM and mixture of ethanol & water as a carrier liquid. From the simulation effect of velocity, initial ice volume fraction, particle diameter and concentration of FPD has been predicted.

2. Mathematical Modeling

To modeling of isothermal ice slurry flow, Eulerian KTGF model is considered in which, domain divided into sufficiently small volumes, but still large enough relative to the individual particle diameter and the equations of motion are averaged over these volumes [16]. In this approach, conservation equations are solved for each phase. In the present work, ice slurry flows are considered to be incompressible and ice particles are assumed to be smooth and spherical.

The continuity equations for both the phases are given as:

$$\frac{\partial}{\partial t}(\alpha_l \rho_l) + \nabla \cdot (\alpha_l \rho_l \vec{v}_l) = 0 \qquad (1)$$

$$\frac{\partial}{\partial t}(\alpha_s \rho_s) + \nabla \cdot (\alpha_s \rho_s \vec{v}_s) = 0 \qquad (2)$$

$$\alpha_l + \alpha_s = 1 \qquad (3)$$

where α, ρ, v are volume fraction, density and velocity respectively. The subscripts l denotes the liquid and s solid phase.

The momentum balance equations for both the phases are given as:

For liquid:

$$\frac{\partial}{\partial t}\left(\alpha_l \rho_l \vec{v}_l\right) + \nabla \cdot \left(\alpha_l \rho_l \vec{v}_l \vec{v}_l\right) = -\alpha_l \nabla P + \nabla \tau_l + \alpha_l \rho_l \vec{g} + \vec{R}_{sl} \quad (4)$$

$$\tau_l = \alpha_l \mu_l \left(\nabla \vec{v}_l + \nabla \vec{v}_l^T\right) + \alpha_l \left(\lambda_l - \frac{2}{3}\mu_l\right)\left(\nabla \vec{v}_l\right)\bar{\bar{I}} \quad (5)$$

For Solid:

$$\frac{\partial}{\partial t}\left(\alpha_s \rho_s \vec{v}_s\right) + \nabla \cdot \left(\alpha_s \rho_s \vec{v}_s \vec{v}_s\right) = -\alpha_s \nabla P + \nabla \tau_s + \alpha_s \rho_s \vec{g} - \nabla P_s + \vec{R}_{ls} \quad (6)$$

$$\tau_s = \alpha_s \mu_s \left(\nabla \vec{v}_s + \nabla \vec{v}_s^T\right) + \alpha_s \left(\lambda_s - \frac{2}{3}\mu_s\right)\left(\nabla \vec{v}_s\right)\bar{\bar{I}} \quad (7)$$

where R, μ ,$\bar{\bar{I}}$ are interfacial forces, viscosity, and unit tensor respectively. λ_s defined as bulk viscosity which is the measure of solid particles resistance to compression and expansion (adopted from Lun et al., 1984 [17]).

$$\lambda_s = \frac{4}{3}\alpha_s \rho_s d_s g_{o,ss}\left(1+e_{ss}\right)\left(\frac{\Theta}{\pi}\right)^{0.5} \quad (8)$$

The solid shear viscosity is calculated as Gidaspow *et al.* 1992 [18].

$$\mu_s = \mu_{s,kin} + \mu_{s,col} \quad (9)$$

where $\mu_{s,kin}$, $\mu_{s,col}$ are the kinetic and collisional viscosities given by following equations.

$$\mu_{s,kin} = \frac{10\rho_s d_s \sqrt{\pi\ \Theta_s}}{96\left(1+e_{ss}\right) g_{o,ss}}\left[1 + \frac{4}{5} g_{o,ss} \alpha_s \left(1+e_{ss}\right) g_{o,ss}\right]^2 \alpha_s \quad (10)$$

$$\mu_{s,col} = \frac{4}{5}\alpha_s \rho_s d_s g_{o,ss}\left(1+e_{ss}\right)\left(\frac{\Theta}{\pi}\right)^{0.5} \quad (11)$$

where d_s, e_{ss}, Θ denotes the solid particle diameter, coefficient of restitution between particles and the granular temperature. $g_{0,ss}$ is the radial distribution function that can also be seen as a probability for interaction between particles and defined by the following equation given by Lun et al., 1984.

$$g_{o,ss} = \left[1 - \left(\frac{\alpha_s}{\alpha_{s,\max}}\right)^{1/3}\right]^{-1} \quad (12)$$

The interfacial forces in the present work include drag, lift and turbulent dispersion force. Drag force has most important role in S-L slurry flow is described by Gidaspow, 1994 [19] in the present work

$$\vec{F}_{D,sl} = K_{sl}\left(\vec{v}_s - \vec{v}_l\right) \quad (13)$$

where $K_{ls}\left(=K_{sl}\right)$ are the interphase momentum exchange coefficients.

When, $\alpha_l > 0.8$

$$K_{sl} = \frac{3}{4} C_D \frac{\alpha_s \alpha_l \rho_l \left|\vec{v}_s - \vec{v}_l\right|}{d_s} \alpha_l^{-2.65} \quad (14)$$

where C_D is the drag force coefficient that is expressed as

$$C_D = \frac{24}{\alpha_l \operatorname{Re}_s}\left[1 + 0.15\left(\alpha_l \operatorname{Re}_s\right)^{0.687}\right] \quad (15)$$

When, $\alpha_l \leq 0.8$

$$K_{sl} = \frac{150\alpha_s^2 \mu_l}{\alpha_l d_s^2} + \frac{1.75\alpha_s \rho_l \left|\vec{v}_l - \vec{v}_s\right|}{d_s} \alpha_l^{-2.65} \tag{16}$$

The lift force on the solid phase is calculate in the present work as

$$\vec{F}_{lift,sl} = C_L \rho_l \alpha_s \left(\vec{v}_l - \vec{v}_s\right) \times \nabla \vec{v}_l \tag{17}$$

$$\vec{F}_{lift,sl} = -\vec{F}_{lift,ls} \tag{18}$$

where, C_L is the lift force coefficient which is assigned to be 0.2. The effects of turbulent dispersion forces which avail the interface turbulent momentum transfer is defined using Burns et al. 2004 [20]. For the modelling of S-L flow, KTGF is adopted in which solid particles are treated as molecular of dense gases. During the random motion, the fluctuating energy of solid particles is described by granular temperature (Θ). The granular temperature is estimated by the following equation of fluctuating energy balance.

$$\frac{3}{2}\left[\frac{\partial}{\partial t}(\rho_s \alpha_s \Theta_s) + \nabla.\left(\rho_s \alpha_s \vec{V}_s \Theta_s\right)\right] = (-p_s \bar{\bar{I}} + \bar{\bar{\tau}}_s) : \nabla \vec{V}_s + \nabla.\left(K_{\Theta_s} \nabla \Theta_s\right) - \gamma_{\Theta m} - 3K_{ls}\Theta_s \tag{19}$$

$$k_{\Theta_s} = \frac{150\rho_s d_s \sqrt{(\Theta\pi)}}{384(1+e_{ss})g_{0,ss}}\left[1 + \frac{6}{5}\alpha_s g_{0,ss}(1+e_{ss})\right]^2 + 2\rho_s \alpha_s^2 d_s (1+e_{ss}) g_{0,ss}\sqrt{\left(\frac{\Theta}{\pi}\right)} \tag{20}$$

$$\gamma_{\Theta m} = \frac{12\left(1-e_{ss}^2\right)g_{0,ss}}{d_s\sqrt{\pi}}\rho_s \alpha_s^2 \Theta_s^{3/2} \tag{21}$$

$$P_s = \alpha_s \rho_s \Theta_s + 2\rho_s (1+e_{ss}) \alpha_s^2 g_{0,ss} \Theta_s \tag{22}$$

where P_s, K_{Θ_s}, $\gamma_{\Theta m}$ denotes the solid pressure, energy diffusion coefficient and collisional dissipation energy respectively.

The per phase $k-\in$ turbulence model is adopted to capture the turbulent in the flow [21].

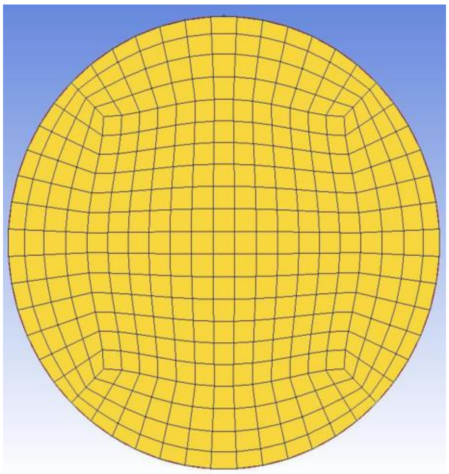

Figure 1 (a). Sketch of meshed pipe cross-section

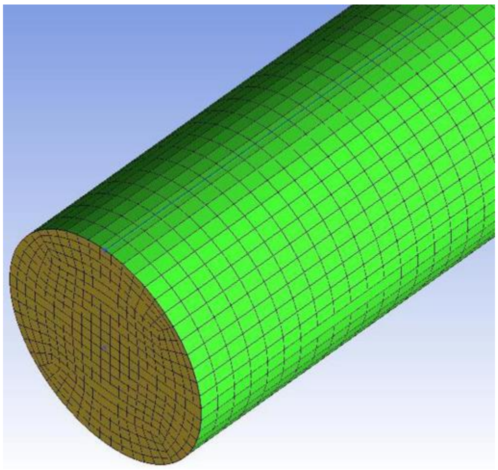

Figure 1 (b). Sketch of meshed pipe

2.1. Boundary Condition & Numerical Procedure

The flow domain is divided into 377000 hexahedron elements by discretising the cross-section into 377 parts (shown in the figure 1.a) and pipe length into 1000 sections (which is shown in the figure

1.b). The grid independence test was also performed, however, further refinement does not influence the results significantly.

The boundary conditions for both the phases are given at inlet, outlet and wall of the pipe. For the inlet, velocity-inlet condition with the velocity perpendicular to the cross-section of the pipe for both the phases and the uniform ice particle volume fraction for solid phase is specified. For the outlet, pressure-outlet condition with zero gauge pressure is specified for both the phases. At the pipe wall, no-slip condition is specified for liquid phase and for the solid phase Johnson-Jackson's condition specified with specularity coefficient of 0.02 and coefficient of restitution 0.9 for particle-wall collision. Finite volume method with SIMPLE algorithm, for coupling pressure and velocity, is applied to solve continuity, momentum and other supporting equations discussed above. All the solutions presented here are calculated for transient condition with time step 0.001 s and converged to residuals of 10^{-4}.

3. Model Validation

Firstly the present model is validated with existing experiment results in literature to ensure that the present model is correct. Figure 1 compares the velocity profiles of slurry flow obtain by the present CFD model and the experimental result of Vuarnoz et al., 2002 in the horizontal pipe of 23 mm diameter, [22]. The results are compared for the ice slurry as a mixture of 10.3 % ethanol in water with particle diameter of 0.1 mm at a velocity of 1.25 m/s. Due to unavailability of experimental data of the ice particle concentration profile, validation is done with the sand-water slurry flow in a horizontal pipe presented by Gillies et al., 2004 [23]. Figure 2 shows the comparison of CFD and experimental results at the mean velocity of 3 m/s, initial sand particle concentration of 19 % and particle diameter of 0.09 mm.

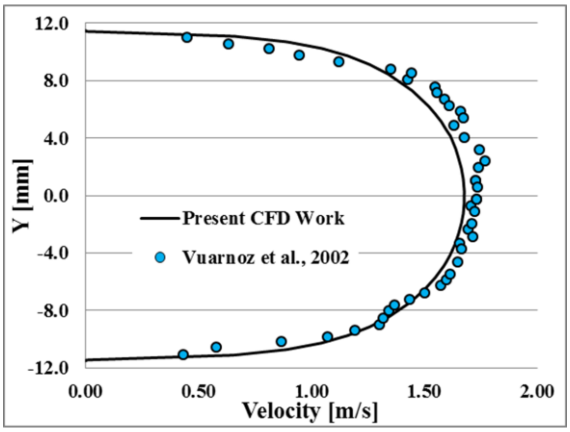

Figure 2. Velocity profile of ice slurry in horizontal pipe

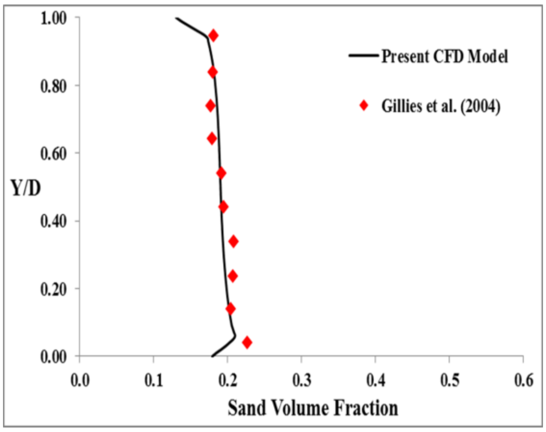

Figure 3. Concentration profile of sand slurry in horizontal pipe

4. Result & Discussion

In ice slurry, ice has a lower density than water and during the flow ice particles try to settle on the top of the pipe due to buoyant force. In ice slurry flow in horizontal pipes, four flows are observed, which classified as: homogeneous, heterogeneous, moving bed and stationary bed flows. Homogeneous flow appears at high velocity and ice particles distribution is uniform. With the decrease in velocity concentration of ice increases towards the top of the pipe and flow is identified as heterogeneous. With the further reduction in velocity the ice concentration at the top reaches to maximum volume fraction and flow regime converts into moving bed. At very low velocity, stationary bed flow occurs in which only liquid flow at the bottom of the pipe and ice particles rest at the top. For the transportation of slurry only homogeneous and heterogeneous conditions are recommended. Therefore, in slurry flow analysis, solid particle distribution is an important parameter which is difficult to measure experimentally.

Figure 4 shows the contours of solid particles distribution at the perpendicular cross section on the outlet of the pipe. The contours of solid particles distribution are shown for the different inlet velocities of 1, 2 and 3 m/s at different initial solid volume fractions of 10, 20 and 30 %. It can be observed from the figure that the distribution of the ice particles is almost homogeneous. The contours are showing that, with the increases in initial volume fractions and inlet velocities the distribution of particle is more uniform due to more frequent particle-particle collisions.

Figure shows that for all initial volume fractions, the maximum value of the local ice volume fraction occurs at the top of the pipe and with the increases of inlet velocity the value of maximum value of the local ice volume fraction lies away from the top pipe due to the repulsive forces from the wall due to particles wall collision. The repulsive force becomes more significant at higher velocity and higher initial volume fraction.

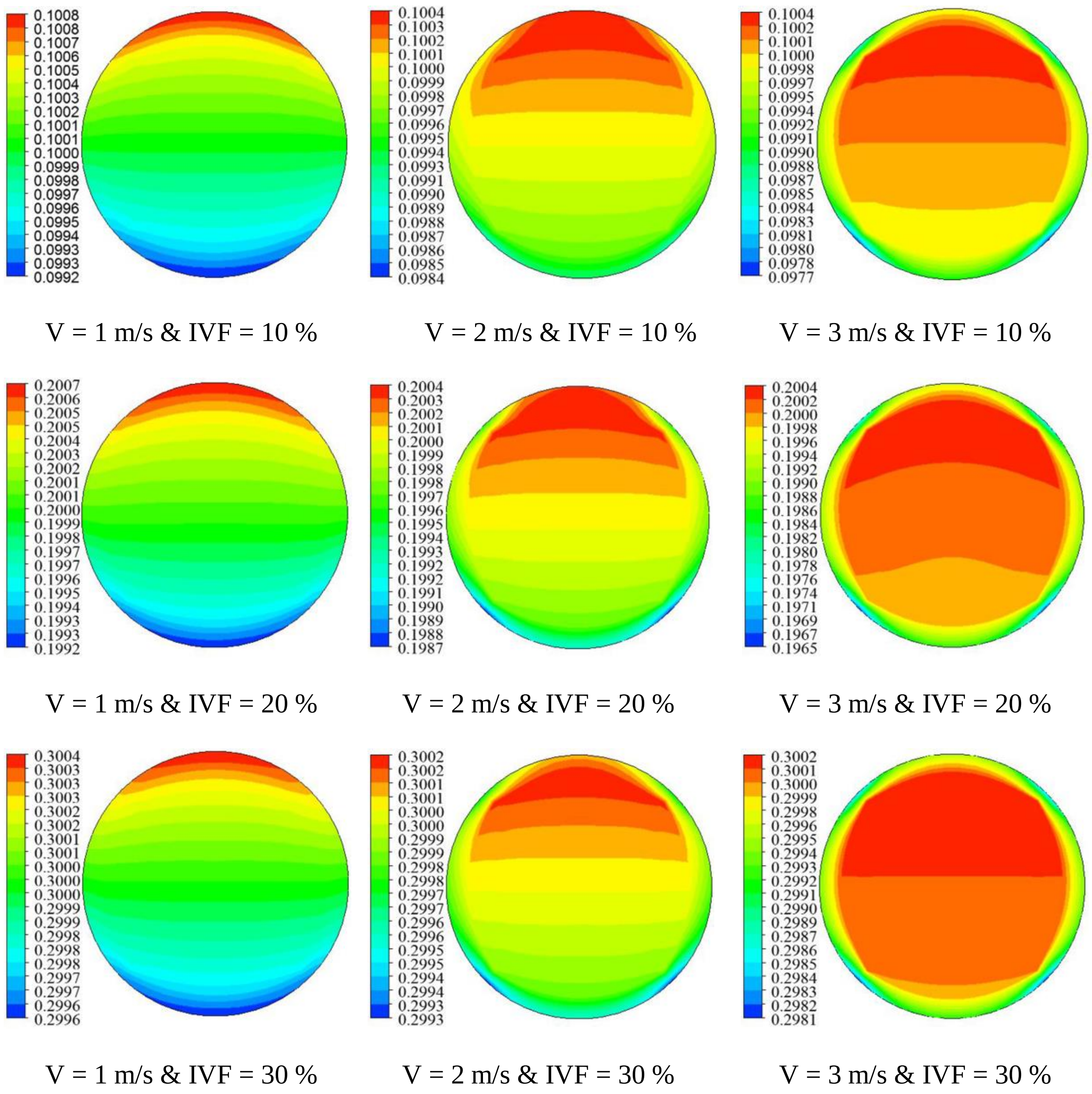

Figure 4. Contours of ice volume fraction at different inlet velocities and initial volume fraction

Effect of particle diameter on concentration profile has been shown in the figure 5. The results are shown for the different particle diameters of 0.1, 0.25 and 0.4 mm at constant inlet velocity of 1 m/s & IVF of 10 %. It can be seen in the figure that as the particle diameter increases the solid concentration increase in the upper half and decrease in the lower half of the pipe; hence flow is more heterogeneous with higher particle diameter. The bigger diameter particles have more inertia to move upward in comparison to small particles, therefore the concentration of ice particles is more at the top with a bigger particles diameter. It can also be observed from the figure that the effect of particle wall collision is more significant with the higher particle diameter due to greater repulsive forces from the wall.

Figure 6 shows the effect of different concentration of FPD in ice slurry on concentration profile. The results are shown for 0, 5 and 10 % of ethanol based ice slurry at constant inlet velocity of 1 m/s & IVF of 10 %. Figure shows that flow became more homogeneous as the concentration of ethanol increases in the solution due to decrease in density difference between solid and liquid phases. However, with the increase of ethanol concentration in the water also reduced the freezing point temperature of the liquid phase. The performance of the ice making unit decreases with lower freezing point liquid, as the evaporator temperature must be lower than freezing point of the liquid to produce ice [24].

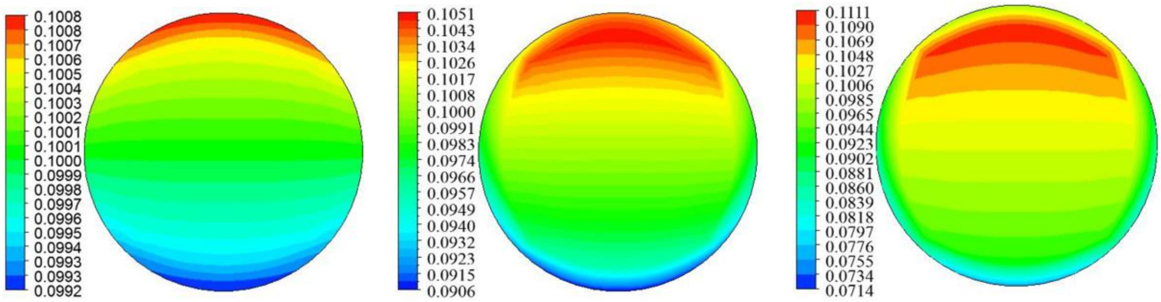

D_p = 0.10 mm D_p = 0.25 mm D_p = 0.40 mm

Figure 5. Contours of ice volume fraction at different particle diameters

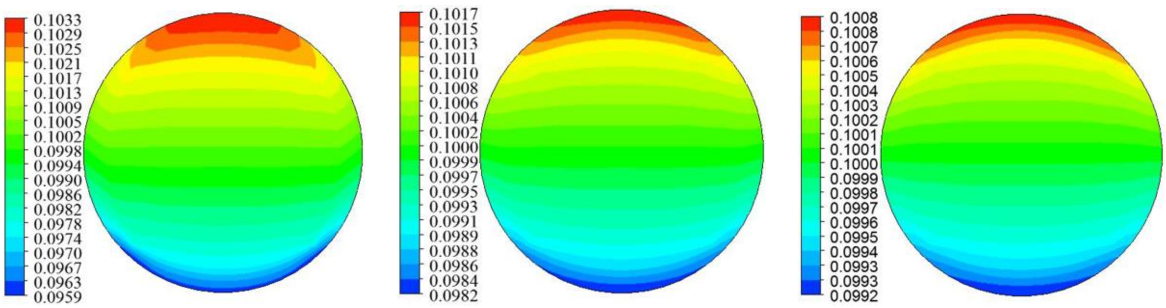

Figure 6. Contours of ice volume fraction at different concentration of ethanol in slurry

Figure 7 shows the contours of the velocity distribution of the solid phase at the perpendicular cross section on the outlet of the pipe. The contours of velocity distribution are shown for the different inlet velocities of 1, 2 and 3 m/s at different initial solid volume fractions of 10, 20 and 30 %. The velocity contours shows that the local velocity near the pipe wall is almost stagnant and has very low value due to viscous forces are dominating near the wall region.

The value of the velocity increases as we move radially toward center. Figure shows that for the constant inlet velocity, the value of local velocity increases with initial volume fraction of ice at the center of the pipe. It is also observed that at constant volume fraction of ice, velocity profile is more homogeneous with increase in inlet velocity. The distribution of the velocity is symmetric for all the cases and it is also observed that there is no difference in the velocity distribution between the solid and liquid phase for all the cases.

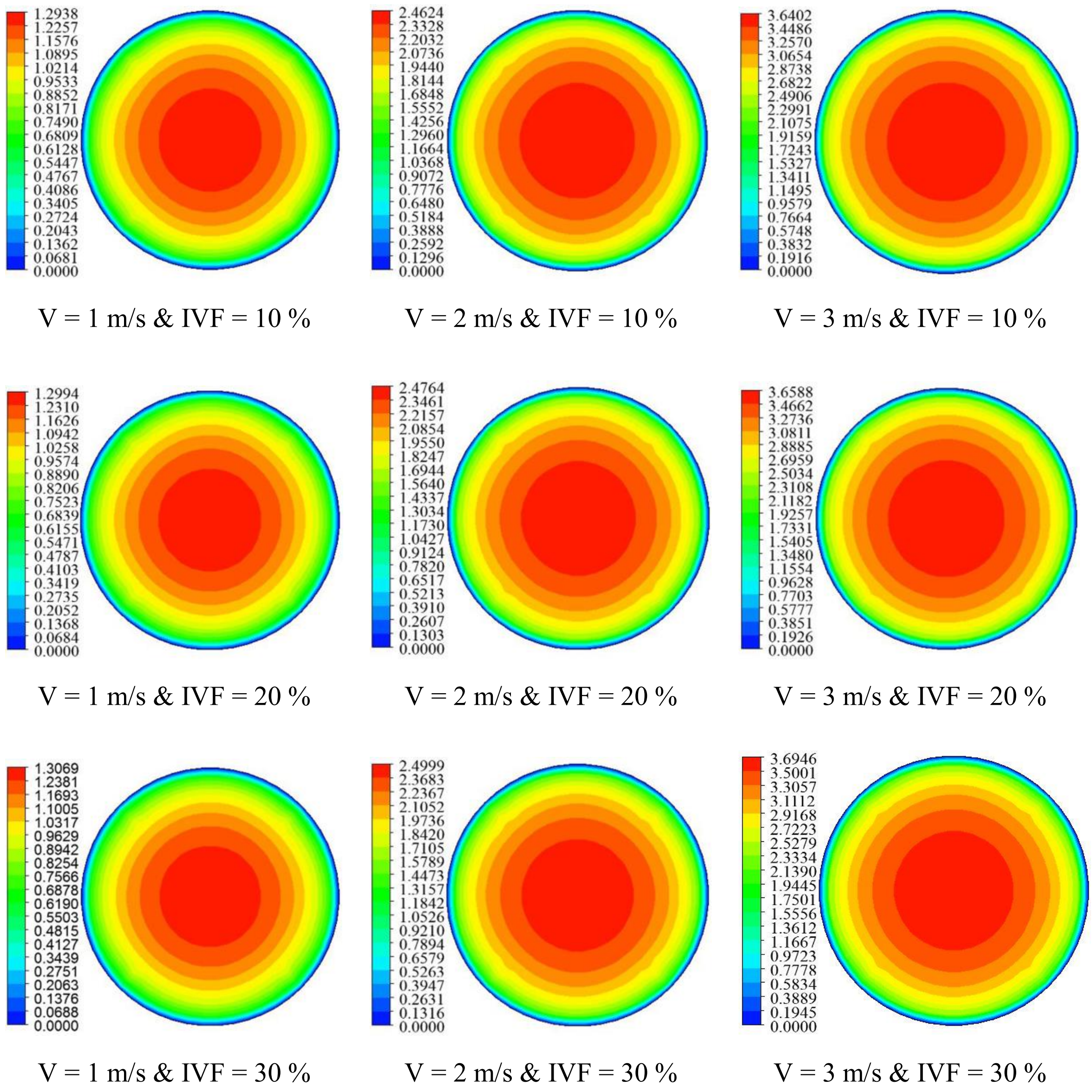

Figure 7. Contours of solid phase velocity at different inlet velocities and initial volume fraction

Figure 8 shows the variation of pressure drop per unit length with the inlet velocity and initial volume fraction. Pressure drop is an important parameter since it is used to determine the pump capacity. The pressure losses in the slurry flow are due to the S-L interaction and the collisions between solid particles & with the wall. Due to increase in velocity and ice concentration, the rate of interaction between S-L, and number of collision particles & wall increases which causes more frictional losses. However the percentage change in the pressure drop with ice fraction is small in comparison to the velocity.

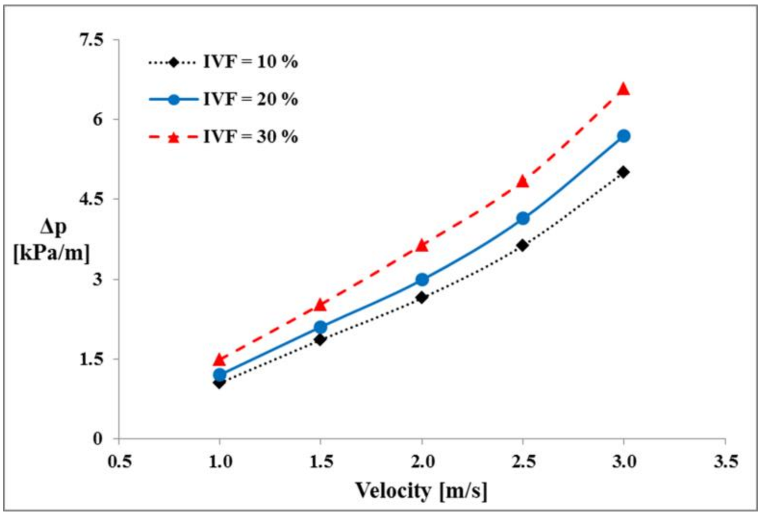

Figure 8. Variation of pressure drop per unit length with velocity and ice volume fraction

5. Conclusions

In the present work, numerical investigation of ice slurry flow has been carried out using Eulerian KTGF model and following conclusions can be inferred from results:

- The distribution of ice particles is uniform for 10 % ethanol based ice slurry with particle diameter of 0.1 mm at the inlet velocity of 1 m/s and 10 % IVF and flow become more homogeneous with increase in inlet velocity and IVF.
- The chance of ice slurry flow to become heterogeneous increases with increase in particles diameter. The repletion forces from the wall is also significant with higher particle diameter and higher inlet velocity and IVF
- Velocity profile for both solid and liquid are same for heterogeneous flow. Velocity profile is symmetric for all the cases due to high velocity and small particle size.
- The variation of pressure drop also investigated in the simulations. Pressure drop increases with increase in velocity and ice concentration due to more interaction between the phases and frequent collision between particles & wall.

6. References

[1] Mahato A, Kumar A. Modeling transport phenomena of ice slurry in an ice forming unit. International Journal of Refrigeration. 2016 Sep 30;69:205-22.

[2] Vakiloroaya V, Samali B, Fakhar A, Pishghadam K. A review of different strategies for HVAC energy saving. Energy Conversion and Management. 2014 Jan 31;77:738-54.

[3] Delgado M, Lázaro A, Mazo J, Zalba B. Review on phase change material emulsions and microencapsulated phase change material slurries: materials, heat transfer studies and applications. Renewable and Sustainable Energy Reviews. 2012 Jan 31;16(1):253-73.

[4] Chandel SS, Agarwal T. Review of current state of research on energy storage, toxicity, health hazards and commercialization of phase changing materials. Renewable and Sustainable Energy Reviews. 2017 Jan 31;67:581-96.

[5] Wang K, Eisele M, Hwang Y, Radermacher R. Review of secondary loop refrigeration systems. International Journal of Refrigeration. 2010 Mar 31;33(2):212-34.

[6] Kauffeld M, Wang MJ, Goldstein V, Kasza KE. Ice slurry applications. International Journal of Refrigeration. 2010 Dec 31;33(8):1491-505.

[7] Shi XJ, Zhang P. Two-phase flow and heat transfer characteristics of tetra-n-butyl ammonium bromide clathrate hydrate slurry in horizontal 90° elbow pipe and U-pipe. International Journal of Heat and Mass Transfer. 2016 Jun 30;97:364-78.
[8] Messa GV, Malin M, Malavasi S. Numerical prediction of fully-suspended slurry flow in horizontal pipes. Powder Technology. 2014 Apr 30;256:61-70.
[9] Niezgoda-Żelasko B, Zalewski W. Momentum transfer of ice slurry flows in tubes, modeling. International Journal of Refrigeration. 2006 May 31;29(3):429-36.
[10] Wang J, Wang S, Zhang T, Liang Y. Numerical investigation of ice slurry isothermal flow in various pipes. International Journal of Refrigeration. 2013 Jan 31;36(1):70-80.
[11] Wang J, Zhang T, Wang S. Heterogeneous ice slurry flow and concentration distribution in horizontal pipes. International Journal of Heat and Fluid Flow. 2013 Dec 31;44:425-34.
[12] Zhang P, Shi XJ. Thermo-fluidic characteristics of ice slurry in horizontal circular pipes. International Journal of Heat and Mass Transfer. 2015 Oct 31;89:950-63.
[13] Jin, T., Li, Y.J., Liang, Z.B., Lan, Y.Q., Lei, G. and Gao, X., 2017. Numerical prediction of flow characteristics of slush hydrogen in a horizontal pipe. International Journal of Hydrogen Energy, 42(6), pp.3778-3789.
[14] Nayak, B.B., Chatterjee, D. and Mullick, A.N., 2017. Numerical prediction of flow and heat transfer characteristics of water-fly ash slurry in a 180° return pipe bend. International Journal of Thermal Sciences, 113, pp.100-115.
[15] Nayak, B.B. and Chatterjee, D., 2017. Numerical investigation of convective heat transfer in pipeline flow of multi-sized mono dispersed fly ash-water slurry. International Journal of Heat and Mass Transfer, 108, pp.1802-1818.
[16] Myerson A. Handbook of industrial crystallization. Butterworth-Heinemann; 2002 Jan 8.
[17] Lun CK, Savage SB, Jeffrey DJ, Chepurniy N. Kinetic theories for granular flow: inelastic particles in Couette flow and slightly inelastic particles in a general flow field. Journal of fluid mechanics. 1984 Mar 1;140:223-56.
[18] Gidaspow D, Bezburuah R, Ding J. Hydrodynamics of circulating fluidized beds: kinetic theory approach. Illinois Inst. of Tech., Chicago, IL (United States). Dept. of Chemical Engineering; 1991 Jan 1.
[19] Gidaspow D. Multiphase flow and fluidization: continuum and kinetic theory descriptions. Academic press; 1994.
[20] Burns AD, Frank T, Hamill I, Shi JM. The Favre averaged drag model for turbulent dispersion in Eulerian multi-phase flows. In5th international conference on multiphase flow, ICMF 2004 May 30 (Vol. 4, pp. 1-17).
[21] Kaushal DR, Thinglas T, Tomita Y, Kuchii S, Tsukamoto H. CFD modeling for pipeline flow of fine particles at high concentration. International Journal of Multiphase Flow. 2012 Jul 31;43:85-100.
[22] Vuarnoz D, Sari O, Egolf PW, Liardon H. Ultrasonic velocity profiler UVP-XW for ice-slurry flow characterisation. InProceedings of the third international symposium on ultrasonic Doppler method for fluid mechanics and fluid engineering, Lausanne, Switzerland 2002 Sep 9.
[23] Gillies RG, Shook CA, Xu J. Modelling heterogeneous slurry flows at high velocities. The Canadian Journal of Chemical Engineering. 2004 Oct 1;82(5):1060-5.
[24] Tian Q, He G, Wang H, Cai D. Simulation on transportation safety of ice slurry in ice cooling system of buildings. Energy and Buildings. 2014 Apr 30;72:262-70.